Supporting Information

Autonomous Chitosan-Based Self-Healing Hydrogel Formed through Non-Covalent Interactions

Zhong-Xing Zhang [*,a], Sing Shy Liow[a], Kun Xue[a], Xikui Zhang[a], Zibiao Li[a], and Xian Jun Loh[*, a,b]

[a] Institute of Materials Research and Engineering, A*STAR (Agency for Science, Technology and Research), 2 Fusionopolis Way, Innovis, #08-03, Singapore 138634, Singapore. Email: zhangzx@imre.a-star.edu.sg; lohxj@imre.a-star.edu.sg ; Tel: +65 6501 1800

[b] National University of Singapore, Department of Materials Science and Engineering, Singapore 117576, Singapore
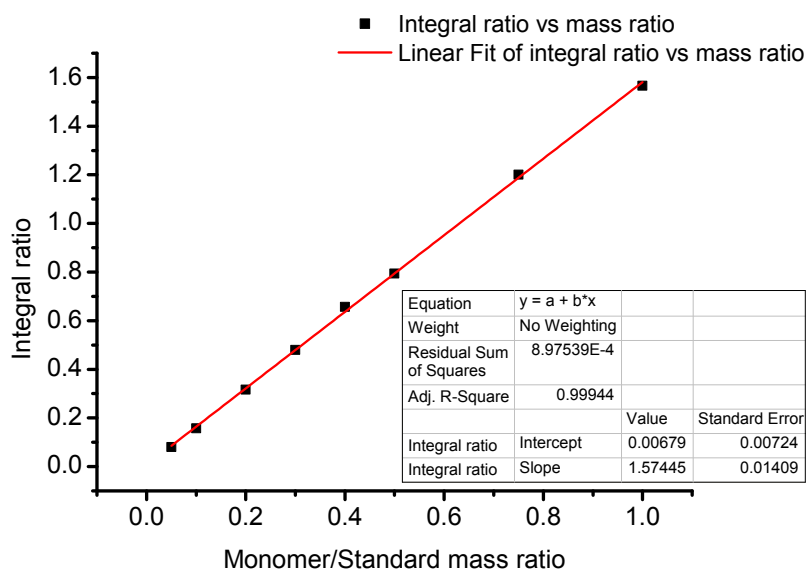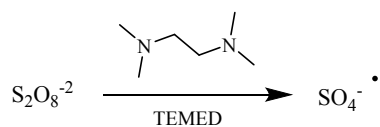
1. Calibration Curve for Monomer Conversion Measurement

Equation	y = a + b*x		
Weight	No Weighting		
Residual Sum of Squares	8.97539E-4		
Adj. R-Square	0.99944		
		Value	Standard Error
Integral ratio	Intercept	0.00679	0.00724
Integral ratio	Slope	1.57445	0.01409

Figure S1. Calibration curve of acrylamide/standard integral ratio versus acrylamide/standard mass ratio based on ^{1}H NMR analysis (DMSO-d_6, 500 MHz, 298K) with decanoic acid as internal standard.
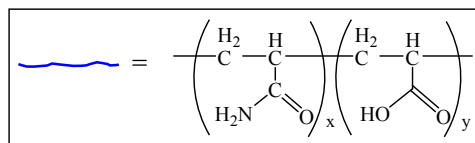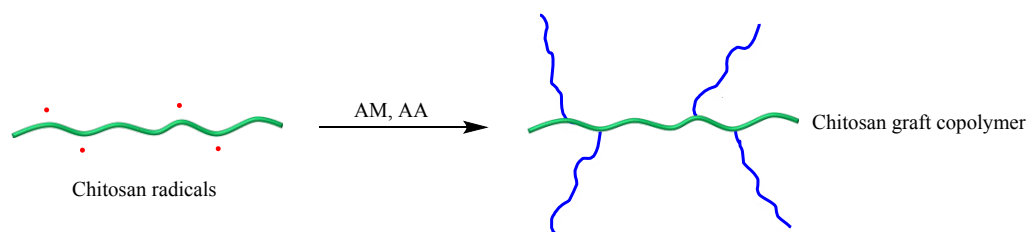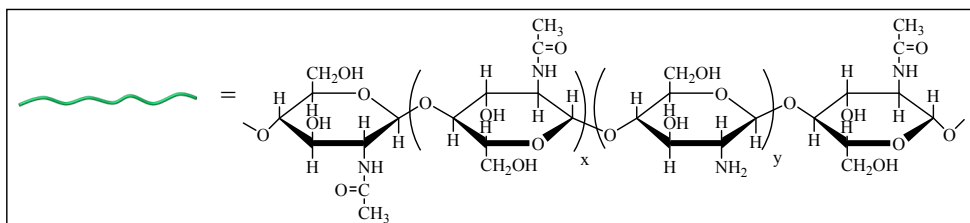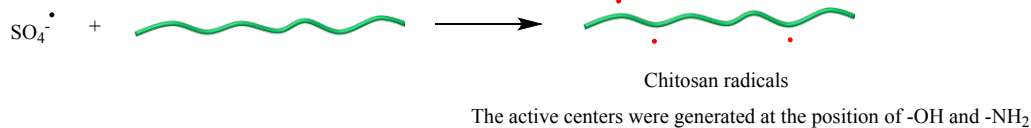
2. Polymerization Mechanism

According to some reported mechanisms in literature,[1-6] the possible initiation and chain growth routes for the formation of chitosan graft copolymers during the preparation of chitosan-based hydrogel were illustrated in Scheme S1.
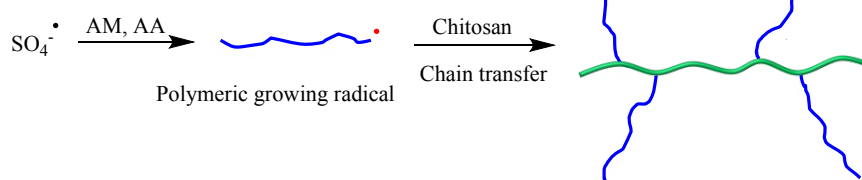
$S_2O_8^{-2}$ $\xrightarrow{\text{TEMED}}$ $SO_4^{-\cdot}$

1. Possible pathways of grafting polymerization:

(1) Grafting from

$SO_4^{-\cdot}$ + ⎰⎱⎰⎱ → ⎰⎱⎰⎱ Chitosan radicals

Chitosan radicals

The active centers were generated at the position of -OH and -NH$_2$

⎰⎱⎰⎱ =

Chitosan radicals $\xrightarrow{\text{AM, AA}}$ Chitosan graft copolymer

(2) Grafting to

$SO_4^{-\cdot}$ $\xrightarrow{\text{AM, AA}}$ Polymeric growing radical $\xrightarrow[\text{Chain transfer}]{\text{Chitosan}}$
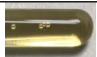
2. An example of potential crosslinking reaction needs to be avoided:

$\xrightarrow[\text{termination}]{\text{Radical coupling}}$
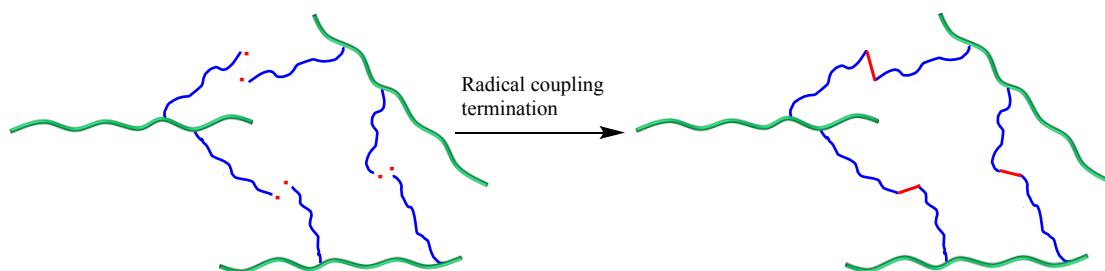
Scheme S1. Schematic depiction of the possible pathways for the formation chitosan graft copolymer during the *in situ* polymerization of AA and AM initiated by APS-TEMED in the presence of chitosan.

3. Characterization Results

Table S1. Appearance, elongation and self-healing properties of the chitosan-based hydrogels prepared with different formulations and conditions

Entry	T (°C)	AA (mol·L⁻¹)	AM (mol·L⁻¹)	APS (mol·L⁻¹)	λ (%)	f (%)	Appearance
1	50	0.076	0.876	0.0148	108 ±11	10±3	
2	40	0.076	0.876	0.0148	182±25	13±1	
3	30	0.076	0.876	0.0148	274 ±15	36±3	
4	22	0.076	0.876	0.0148	442±12	44±2	
5	30	0.150	0.798	0.0148	186±7	0	
6	30	0.112	0.836	0.0148	214±28	0	
7	30	0.056	0.893	0.0148	277±33	39±2	
8	30	0	0.950	0.0148	278±31	49±1	
9	30	0.056	0.893	0.0148	278±44	44±3	
10	30	0.056	0.893	0.0119	344±15	61±3	
11	30	0.056	0.893	0.00741	368±2	67±3	
12	30	0.056	0.893	0.00444	442±12	71±3	
13	30	0.056	0.893	0.00296	625±35	88±3	
14	30	0.056	0.893	0.00222	844 ±16	91±7	

*Chitosan concentration: 2.25 wt%; TEMED: 0.0167 mol·L⁻¹.

λ: the percentage elongation at break of the original hydrogel sample.

f : the healing efficiency.

Samples of entry 7 and entry 9 were prepared using identical formulation under identical conditions.

3.1 Effect of the polymerization temperature

Polymerization temperature will have great effect on the hydrogel's self-healing ability because of the existence of potential chain coupling termination during the *in situ*

polymerization which will cause chemical crosslinking of the chitosan graft copolymer. To perform the *in situ* polymerization at lower temperatures can effectively suppress the occurrence of the chemical crosslinking. The variations of the healing efficiency (*f*) of the resultant hydrogels versus polymerization temperature (entries 1-4 in Table S1) were shown in Figure S2.
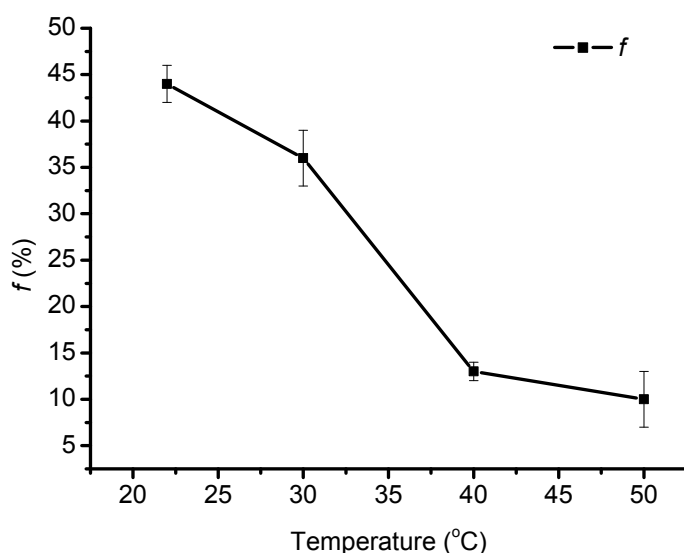
Figure S2. The variations of the healing efficiency (*f*) of the resultant hydrogels as a function of polymerization temperature. Formulation: Chitosan 2.25 wt%, AA 0.076 mol·L^{-1}, AM 0.876 mol·L^{-1}, APS 0.0148 mol·L^{-1}, TEMED 0.0167 mol·L^{-1}. Polymerization for 24 h. Each point represents the mean value ± SD.

3.2 Effect of the feeding amount of acrylic acid

The variations of the healing efficiency (*f*) of the resultant hydrogels versus initial AA/AM molar ratio were shown in Figure S3 (a). The relationship between the rheological property of hydrogels and the initial AA/AM molar ratio was shown in Figure S3 (b) (refer to entry 3 and entries 5-8 in Table S1 for formulations).
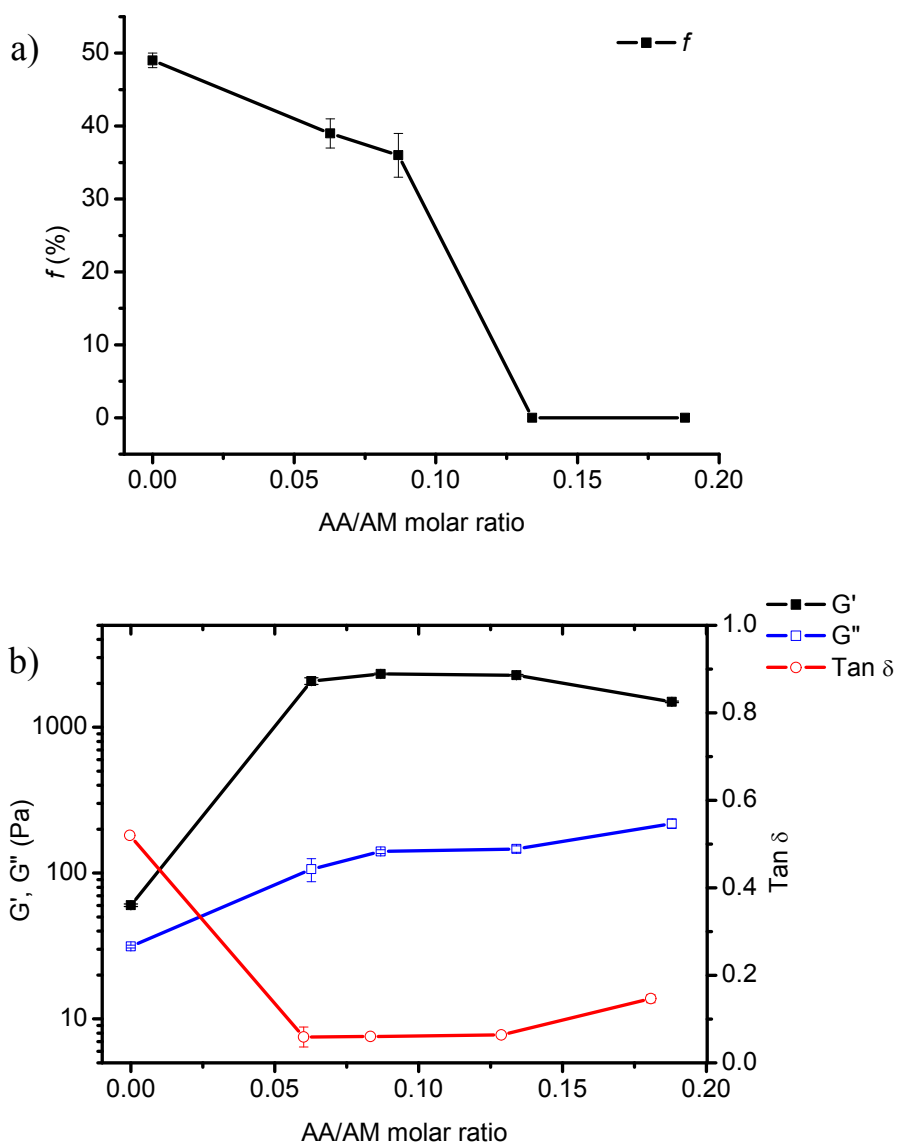
Figure S3. (a) The variations of the healing efficiency (*f*) of the resultant hydrogels as a function of initial AA/AM molar ratio. (b) The variations of the storage modulus (G'), loss modulus (G") and Tan δ of the resultant hydrogels as a function of initial AA/AM molar ratio at constant angular frequency ω of 10 rad/s and strain of 1.0 % at 25 °C. Formulation: Chitosan 2.25 wt%, total monomer concentration kept around 0.95 mol·L^{-1}, APS 0.0148 mol·L^{-1}, TEMED 0.0167 mol·L^{-1}. Polymerization at 30 °C for 24 h. Each point represents the mean value ± SD.

3.3 Effect of the feeding amount of APS

The variations of the healing efficiency (*f*) of the resultant hydrogels vesus initial ammonium persulfate (APS) concentrations (entries 9-14 in Table S1) were shown in Figure S4.
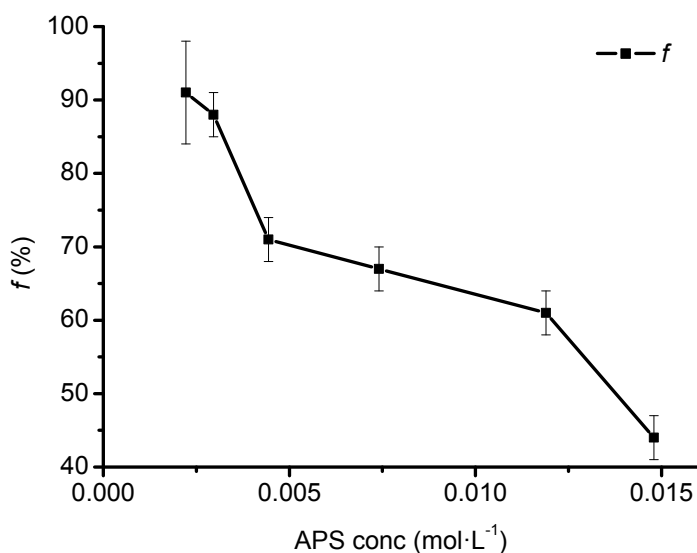
Figure S4. The variations of the healing efficiency (*f*) of the resultant hydrogels as a function of initial ammonium persulfate (APS) concentrations. Formulation: Chitosan 2.25 wt%, AA 0.056 mol·L^{-1}, AM 0.893 mol·L^{-1}, TEMED 0.0167 mol·L^{-1}. Polymerization at 30 °C for 24 h. Each point represents the mean value ± SD.

3.4 Characterization of representative hydrogel sample

A representative hydrogel (entry 13 in Table S1) was further studied and characterized.

(1) Monomer conversion, hydrogel composition and molecular weight of chitosan graft copolymer

Table S2. Monomer conversion for the representative hydrogel, the hydrogel composition analysis, and the estimated molecular weight of chitosan graft copolymer [a]

Monomer conversion (%)[b]	Solid content (%)[c]	Residual acrylamide content (%)[d]	Solid content after purification (%)[e]	Non- grafted polymer content (%)[f]	Mn (g/mol)[g]
94.6 ± 0.7	9.6 ± 0.4	0.35 ± 0.05	9.0 ± 0.3	0.25	150 K (PDI 2.0)

[a] Refer to Table S1, entry 13 for the formulations and conditions.

[b] Calculated by ^{1}H NMR spectroscopy based on the determination of residual acrylamide in final hydrogel.

[c] Solid content = $W_d / W_o \times 100\%$, where W_o is the original weight of the hydrogel sample, and W_d is the weight of the hydrogel sample after dried in vacuum oven at 50 °C for 2 days.

[d] Calculated according to calibration curve (Figure S1).

[e] Solid content after purification = $W_d'/ W_o \times 100\%$, where W_o is the original weight of the hydrogel sample, and W_d' is the weight of the hydrogel sample after purification and dried in vacuum oven at 50 °C for 2 days.

[f] Non-grafted polymer content = (Solid content) − (Solid content after purification) − (Residual acrylamide content)

[g] The estimated molecular weight of chitosan graft copolymer and polydispersity index (PDI) was according to SEC test using HOAc-NaOAc (0.3 M/0.2 M) buffer as eluent.

(2) FTIR

Figure S5 shows the FTIR spectra of the representative hydrogel and pure chitosan (CS). The FT-IR spectrum of CS exhibits the characteristic peaks at 3445 cm^{-1} (O-H stretch), 2883 cm^{-1} (C-H stretch), 1652 cm^{-1} (O-H bending), 1000 − 1250 cm^{-1} (C-O and C-O-H stretch). FTIR spectrum of the hydrogel shows additional distinct bands at 1720 and 1671 cm^{-1} which correspond to C=O stretching vibration of the -COOH and –CONH$_2$ groups in synthetic polymeric chains. The additional bands at 2973 and 2934 cm^{-1} are assigned to the asymmetric -CH$_3$ and -CH$_2$, respectively.
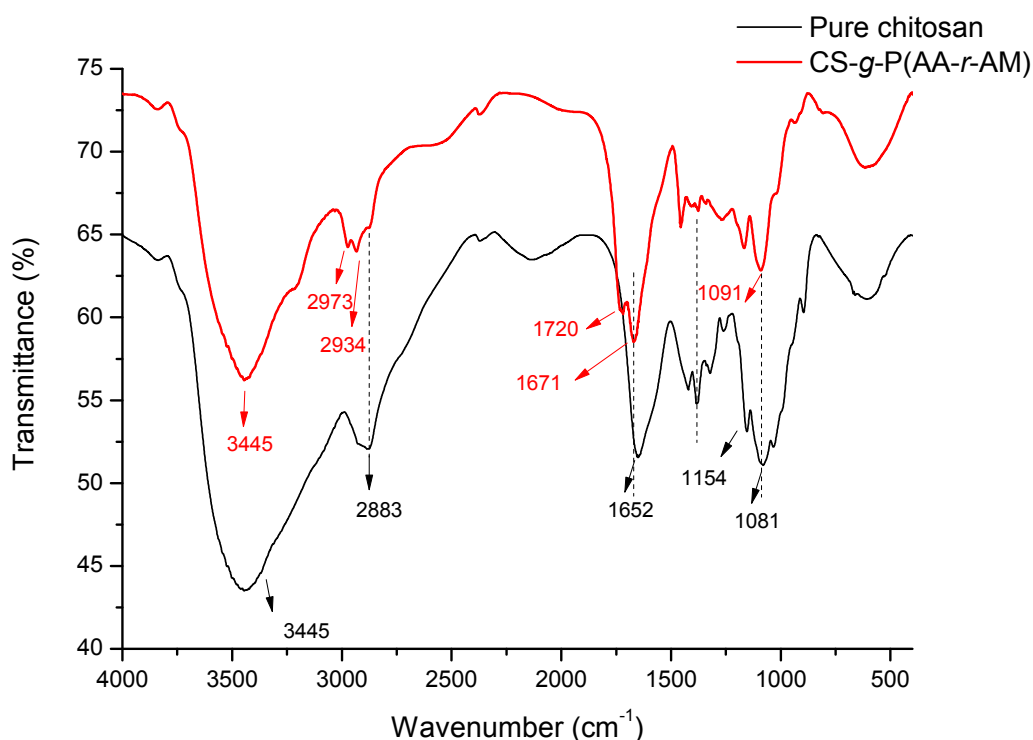

Figure S5. FTIR spectra of the dried representative hydrogel and pure chitosan (CS) recorded at room temperature.
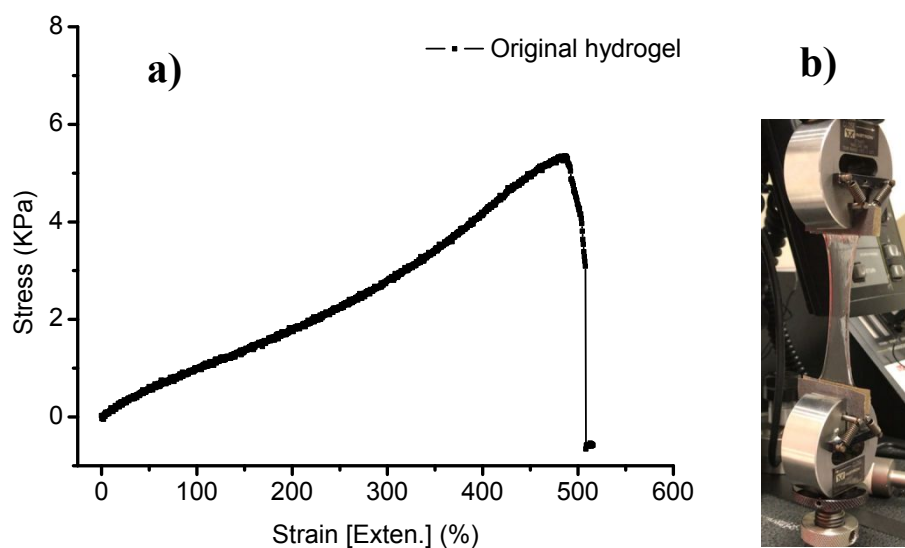
(3) Tensile test

Figure S6. (a) A typical tensile stress-strain curve for original hydrogel sample recorded at room temperature. (b) A photo of the hydrogel sample during tensile test.
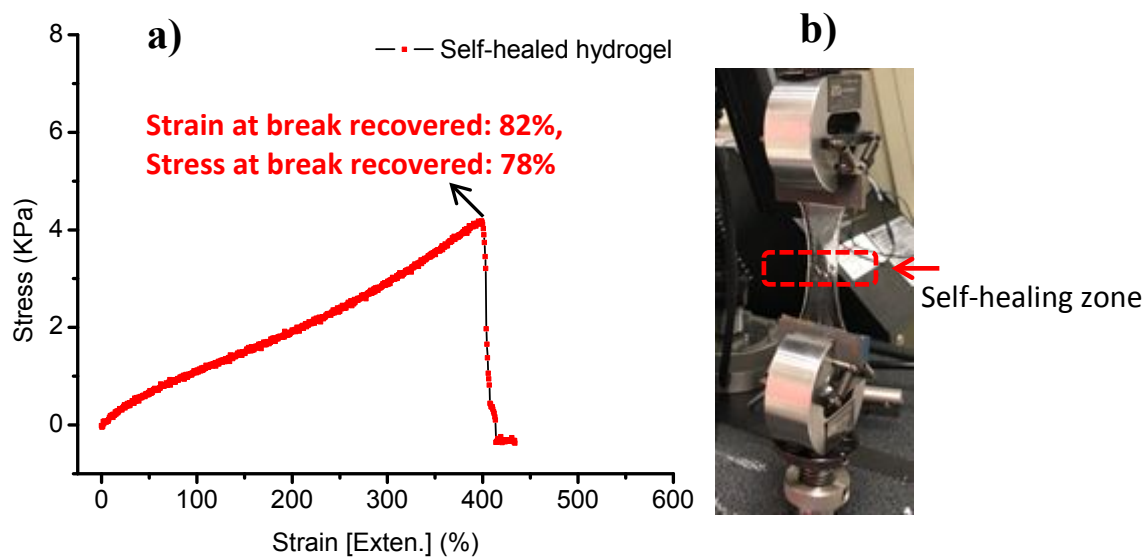

Figure S7. (a) A typical tensile stress-strain curve for self-healed hydrogel sample recorded at room temperature. (b) A photo of the hydrogel sample during tensile test.
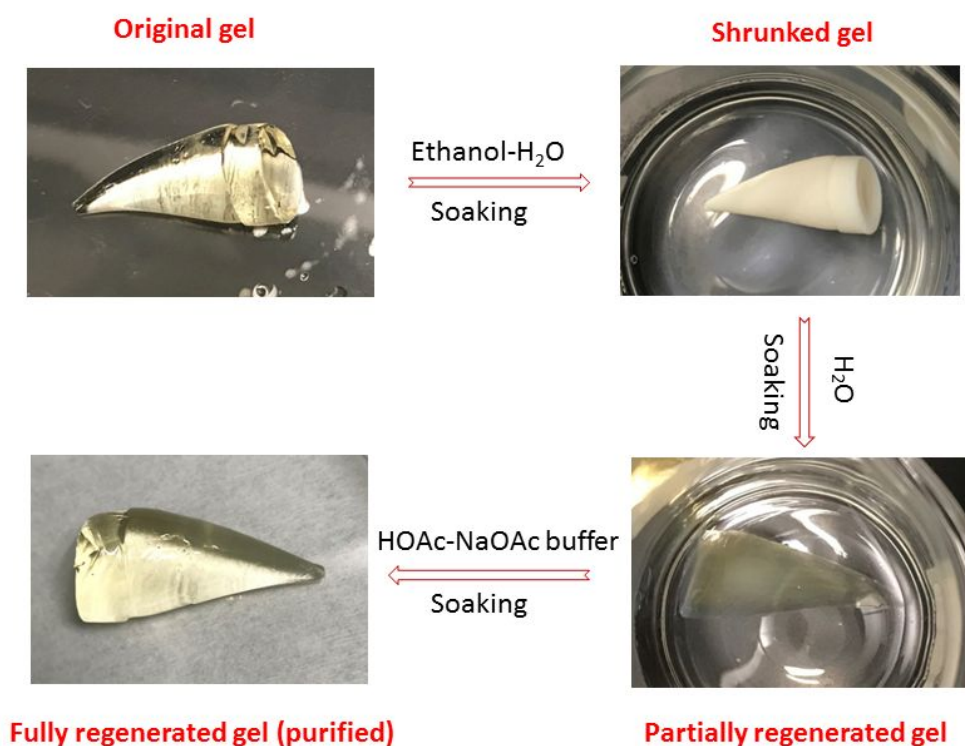
(4) Purification and regeneration

Figure S8. A typical hydrogel purification and regeneration process by successively soaking the hydrogel in ethanol-H_2O (1/1, v/v), pure H_2O and HOAc-NaOAc buffer (0.1 M, pH 4.5) at room temperature.

(5) Dissolution test

Table S3. Dissolution of hydrogel samples under different conditions [a]

Entry	Conditions	Results
1	Dilute HCl aq. (1.0 M), 40 °C, stirring, 2h	Completely dissolved
2	Dilute HCl aq. (0.2 M), 40 °C, stirring, 2h	Completely dissolved
3	Dilute HOAc aq. (0.2 M), 40 °C, stirring, 2h	Completely dissolved
4	Dilute NaOH aq. (0.2 M), 40 °C, stirring, 4h	Not dissolved

[a] Typically, 25 mg of hydrogel sample was treated with 2 mL of acidic or basic solution.

References

1.   Strachota, B.; Matejka, L.; Zhigunov, A.; Konefal, R.; Spevacek, J.; Dybal, J.; Puffr, R.,
Poly(N-isopropylacrylamide)-clay based hydrogels controlled by the initiating conditions: evolution
of structure and gel formation. *Soft Matter* **2015,** *11* (48), 9291-9306.

2.   Hu, X. B.; Tong, Z.; Lyon, L. A., Control of Poly(N-isopropylacrylamide) Microgel Network
Structure by Precipitation Polymerization near the Lower Critical Solution Temperature. *Langmuir*
2011, *27* (7), 4142-4148.

3.   Al-Karawi, A. J. M.; Al-Qaisi, Z. H. J.; Abdullah, H. I.; Al-Mokaram, A. M. A.; Al-Heetimi,
D. T. A., Synthesis, characterization of acrylamide grafted chitosan and its use in removal of
copper(II) ions from water. *Carbohydr. Polym.* **2011,** *83* (2), 495-500.

4.   Recillas, M.; Silva, L. L.; Peniche, C.; Goycoolea, F. M.; Rinaudo, M.; Arguelles-Monal, W.
M., Thermoresponsive Behavior of Chitosan-g-N-isopropylacrylamide Copolymer Solutions.
Biomacromolecules **2009,** *10* (6), 1633-1641.

5.   Mahdavinia, G. R.; Pourjavadi, A.; Hosseinzadeh, H.; Zohuriaan, M. J., Modified chitosan 4.
Superabsorbent hydrogels from poly(acrylic acid-co-acrylamide) grafted chitosan with salt- and pH-
responsiveness properties. *European Polymer Journal* **2004,** *40* (7), 1399-1407.

6.   Peniche, C.; Arguelles-Monal, W.; Davidenko, N.; Sastre, R.; Gallardo, A.; San Roman, J.,
Self-curing membranes of chitosan/PAA IPNs obtained by radical polymerization: preparation,
characterization and interpolymer complexation. *Biomaterials* **1999,** *20* (20), 1869-1878.